PhCN$_3$S$_2$ system exists as a cofacially bonded dimer, with an S---S separation of 2.53 Å. MNDO calculations on model RCN$_3$S$_2$ rings reveal that they possess triplet ground states. The formation of dimeric dithiatriazines arises from the coupling of two such triplets to form a singlet ground state. The structural consequences of modification of the phenyl ring of **4** on the singlet/triplet balance is currently being investigated, as is the effect of redox changes on the stability of the (PhCN$_3$S$_2$)$_2$ structure.

Registry No. 3, 98990-61-5; **4**, 98990-55-7; **5**, 98990-56-8; **6**, 98990-57-9; **7**, 99016-48-5; PhC(N(SiMe$_3$)$_2$)NSiMe$_3$, 24261-90-3; S$_3$N$_3$Cl$_3$, 5964-00-1; Me$_3$SiNSNSiMe$_3$, 18156-25-7; HCN$_3$S$_2$, 33982-51-3; (HC-N$_3$S$_2$)$_2$, 98990-58-0; H$_2$NCN$_3$S$_2$, 98990-59-1; FCN$_3$S$_2$, 98990-60-4; triphenylstibine, 603-36-1; norbornadiene, 121-46-0.

Supplementary Material Available: Tables of atom coordinates for hydrogen atoms (S1) and anisotropic thermal parameters (S2) and observed and calculated structure factors (17 pages). Ordering information is available on any current masthead page.

Theoretical Probes of Activated-Complex Structure and Properties: Substituent Effects in Carbonyl Addition

Ian H. Williams,[1a] Dale Spangler,[1b] Gerald M. Maggiora,*[1c,d] and Richard L. Schowen*[1c]

Contribution from the Departments of Chemistry and Biochemistry, University of Kansas, Lawrence, Kansas 66045-2112, the University Chemical Laboratory, Cambridge CB2 1EW, UK, and the Lawrence Berkeley Laboratory, Berkeley, California 94720. Received May 6, 1985

Abstract: Structures, force fields, vibrational eigenvalues and eigenvectors, potential energies, and Gibbs free energies have been calculated by ab initio quantum-mechanical methods for the reactants, products, and activated complexes of five carbonyl-addition reactions, namely the addition of water, methanol, and ammonia to formaldehyde and the addition of water to acetaldehyde and formyl fluoride. All activated complexes have four-membered ring structures, and the reaction-coordinated eigenvectors show heavy-atom reorganization and proton transfer to be truly concerted in all cases. The structures of the activated complexes are essentially invariant to substitution, the Pauling bond order of the forming carbon-nucleophile bond being 0.42-0.45 and the Pauling bond order of the breaking OH or NH bond being 0.76-0.78 in all cases. Heavy-atom reorganization is thus more advanced than proton transfer in all activated complexes. Potential energies of reaction vary from -4.7 to -17.3 kcal mol^{-1} and potential energies of activation from 35.6 to 46.2 kcal mol^{-1}. Gibbs free energies of reaction vary from -3.0 to +7.6 kcal mol^{-1} and Gibbs free energies of activation from 46.4 to 57.6 kcal mol^{-1}. In neither case is there a systematic relationship between rate and equilibrium energetics. Reaction progress of proton transfer is ~25% and that for heavy-atom reorganization ~45% at the activated complex. Both of these features can be derived from the qualitative location of the activated complex on an MAR. This was arrrived at by deduction of the parallel effect from the exothermicity of the reactions and of the perpendicular effect from reactant frontier-orbital interactions.

An important current goal of mechanisms chemistry, particularly of the subfield of physical-organic chemistry, is the establishment of generalizations which govern the structure and properties (e.g., energy, charge distribution, force constants) of activated complexes under the influence of experimental variables such as substituents, solvent, etc. Successful generalizations of this kind would allow the a priori calculation of the rate of a reaction under various conditions and would be fundamentally important and practically useful.

Progress in this direction is now being made experimentally by the application to systems of interest of mechanistic probes such as substituent effects, medium effects, and isotope effects. The results are generally interpreted in terms of activated-complex structure. Typically, the slope of a linear free-energy plot or the magnitude of a kinetic isotope effect is used to estimate properties of the activated complex, such as the bond orders of forming or breaking bonds. Then the results of several such studies are used to infer the behavior of the activated complex under different conditions. While this approach has yielded considerable mechanistic information, it relies heavily on empirical relationships and concepts.

Theoretical chemistry has a significant potential for contributing to this area in several ways. The approach chosen here has been to *simulate* a typical experimental structure-reactivity study of the type described above. The reactions of a series of substituted compounds have been examined, with reactant, activated complex, and product structures and properties being determined in each case. Since free energies of all species are calculated, rate-equilibrium free-energy relationsips can be constructed; and since force constants of all species are calculated, isotope effects can be obtained. In contrast to experimental studies, however, the theoretical procedures also yield directly the structures and other properties of all species, including the activated complex. The calculated structures and properties can then be compared with those inferred from free-energy relationships or isotope effects. Thus, this approach has the capacity for testing the empirical relationships, developing the principles behind them, and establishing new and more reliable generalizations for use in interpreting experimental results.

In this paper, we report the response of reactant, product and activated-complex properties to variations of substituent in the prototypical carbonyl-addition reaction we have studied previously.[2-4]

Effects of substituents were examined for both the nucleophilic and electrophilic reaction partners. All reactions studied proceed
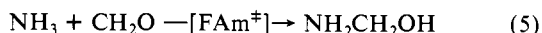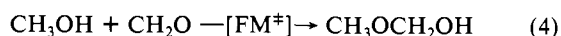
(1) (a) Royal Society Pickering Research Fellow, University of Cambridge. Present address: School of Chemistry, University of Bristol. (b) NRCC. Present address: Molecular Design, Ltd., Hayward, CA. (c) University of Kansas. (d) Present address: The Upjohn Company, Kalamazoo, Michigan.
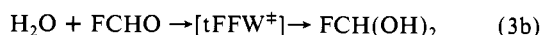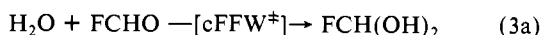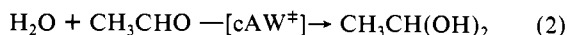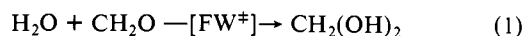
(2) Williams, l. H.; Spangler, D.; Femec, D. A.; Maggiora, G. M.; Schowen, R. l.. *J. Am. Chem. Soc.* **1980**, *102*, 6619.
(3) Williams, I. H.; Maggiora, G. M.; Schowen, R. L. *J. Am. Chem. Soc.* **1980**, *102*, 7831.
(4) Spangler, D.; Williams, I. H.; Maggiora, G. M. *J. Comput. Chem.* **1983**, *4*, 524.

through a single four-center activated complex in a single elementary step (eq 1–5). Three electrophiles (formaldehyde, ac-

$$H_2O + CH_2O \; -[FW^\ddagger] \rightarrow \; CH_2(OH)_2 \qquad (1)$$

$$H_2O + CH_3CHO \; -[cAW^\ddagger] \rightarrow \; CH_3CH(OH)_2 \qquad (2)$$

$$H_2O + FCHO \; -[cFFW^\ddagger] \rightarrow \; FCH(OH)_2 \qquad (3a)$$

$$H_2O + FCHO \; \rightarrow [tFFW^\ddagger] \rightarrow \; FCH(OH)_2 \qquad (3b)$$

$$CH_3OH + CH_2O \; -[FM^\ddagger] \rightarrow \; CH_3OCH_2OH \qquad (4)$$

$$NH_3 + CH_2O \; -[FAm^\ddagger] \rightarrow \; NH_2CH_2OH \qquad (5)$$

etaldehyde, and formyl fluoride) and three nucleophiles (water, methanol, and ammonia) were examined in several combinations, passing through the activated complexes designated[5] FW‡, cAW‡, cFFW‡, tFFW‡, FM‡, and FAm‡.

Computational Methods

Ab initio SCF–MO calculations were performed with versions of the HONDO program[6] as implemented on a VAX 11/780 computer at the National Resource for Computation in Chemistry and on an IBM 370/165 at the Cambridge University Computing Service. Geometry optimizations for reactant and product species were accomplished by using a variant of the quasi-Newton variable metric method[7] with a Broyden-Fletcher-Goldfarb-Shanno Hessian update scheme.[8] Activated-complex structures were determined with use of a novel algorithm described elsewhere.[4] The STO-3G minimal basis[9] was used for all geometry optimizations, and the 4-31G split-valence basis[10] was used for energy calculations for STO-3G optimized structures; such calculations we will refer to by the notation 4-31G//STO-3G. Geometry optimization was continued until the largest component of the gradient vector was in each case less than 10^{-4} hartree bohr^{-1} ($<824\mu$dyne) and convergence of 10^{-9} on the density matrix was achieved in order to obtain sufficient accuracy in analytical gradients.

An earlier study[4] of basis-set effects upon formaldehyde hydration via FW‡ clearly demonstrated that optimized geometries obtained with a minimal STO-3G basis, with a split-valence 4-31G basis, and with an extended split-valence 6-31G** basis were very similar. It was thus concluded that an STO-3G basis was quite adequate for the prediction of essential geometrical features. A similar assumption is justified in the present work by the similarity of these systems to the water–formaldehyde system. The earlier study[4] also demonstrated that energies of reaction were exaggerated by a factot of about 3 in STO-3G in comparison to the two split-valence bases. It is for this reason that we have chosen to carry out geometry optimizations in the simpler STO-3G basis while evaluating the energies in the split-valence 4-31G basis (vide supra). Moreover, it is not expected that inclusion of electron correlation would materially change any conclusions derived from
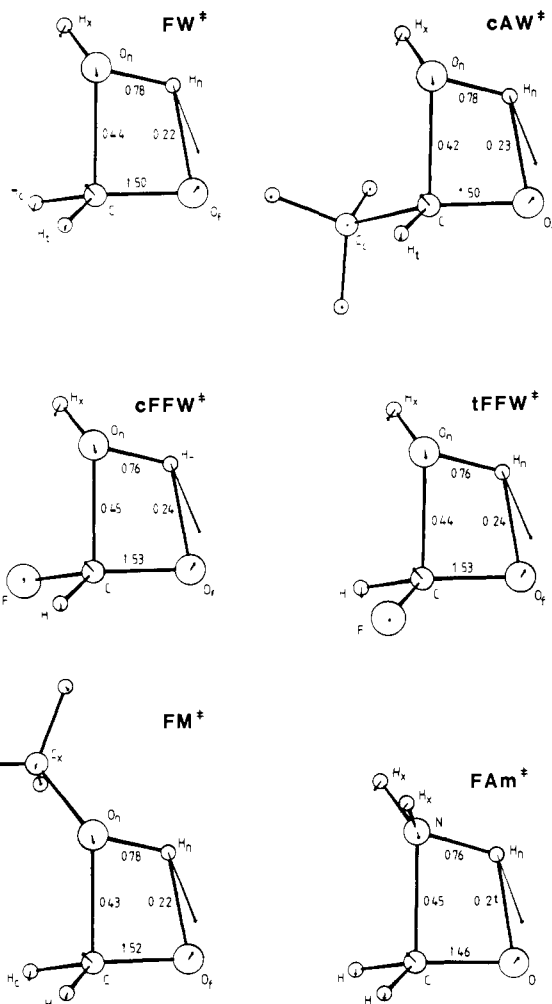

Figure 1. Geometrical structures of activated complexes for the reactions of eq 1–5 {FW‡ (formaldehyde–water), cAW‡ (*cis*-acetaldehyde–water), cFFW‡ (*cis*-formyl fluoride–water), tFFW‡ (*trans*-formyl fluoride–water), FM‡ (formaldehyde–methanol), FAm‡ (formaldehyde–ammonia) [see ref 5 for a fuller description]}.

our current calculations. This assumption is based upon the extensive work of Oie et al.[11-13] on a closely related system, where it was shown that energetic changes due to the inclusion of higher level basis sets (e.g., 6-31G**) and to the inclusion of electron correlation almost perfectly cancel one another.

Force constants were computed in STO-3G by numerical forward-differencing of analytical gradients for geometries displaced in turn by 0.01 bohr in each Cartesian coordinate. Spurious translational and rotational contributions to the Cartesian force constants were projected out,[14] and all the force constants were scaled by a factor of 0.68 (a value which minimizes the root-mean-square error between calculated and observed vibrational frequencies for the reactant molecules and their various isotopomers[15]). Relative Gibbs free energies were calculated at 25 °C according to eq 6, where E is the 4-31G//STO-3G potential

$$\Delta G° = \Delta E + \Delta E_{zp} - RT\Delta \ln (q_t°q_rq_v) \qquad (6)$$

energy, E_{zp} is the zero-point energy, q_t, q_r, and q_v are molecular partition functions for translational, rotational, and vibrational motions (assumed to be separable), and the superscript zero refers

(5) The following notation is adopted for the activated complexes of the various reactions (indicated on the arrows in eq 1–5). Except for the prefixes c and t, the first element is an abbreviation for the electrophile (F: formaldehyde, A: acetaldehyde, FF: formyl fluoride). The second element is an abbreviation for the nucleophile (W: water; M: methanol; Am: ammonia). The superscript $\ddagger$ identifies the structure as an activated complex. The prefix c indicates a cis (approximately synperiplanar) relationship of the exocyclic hydrogen of the nucleophile to the non-hydrogen formyl substituent. The prefix t indicates a trans (approximately anticlinal) relationship of the same two groups. In previous papers,[2,3] where different numbers of nucleophile molecules were present, the number of nucleophile molecules was shown after the abbreviation for the nucleophile (FW1$\ddagger$, FW2$\ddagger$, etc.).

(6) King, H. F.; Dupuis, M.; Rys, J. *Natl. Resourc. Comput. Chem. Software Cat.*, **1980**, 1, Prog. No. QH02 (HONDO).

(7) Fletcher, R. "Practical Methods of Optimization: Unconstrained Optimization"; Wiley: New York, 1980; Vol. 1.

(8) (a) Broyden, C. G. *Math. Comp.* **1970**, *24*, 365. (b) Fletcher, R. *Comput. J.* **1970**, *13*, 317. (c) Goldfarb, D. *Math. Comp.* **1970**, *24*, 23. (d) Shanno, D. *Math. Comp.* **1970**, *24*, 647.

(9) Hehre, W. J.; Stewart, R. F.; Pople, J. A. *J. Phys. Chem.* **1969**, *51*, 2657.

(10) Ditchfield, R.; Hehre, W. J.; Pople, J. A. *J. Chem. Phys.* **1971**, *54*, 724.

(11) Oie, T.; Loew, G. H.; Burt, S. K.; Binkley, J. S.; MacElroy, R. D. *Int. J. Quantum Chem.: Quantum Chem. Symp.* **1982**, *9*, 224.

(12) Oie, T.; Loew, G. H.; Burt, S. K.; Binkley, J. S.; MacElroy, R. D. *J. Am. Chem. Soc.* **1982**, *104*, 6169.

(13) Oie, T.; Loew, G. H.; Burt, S. K.; MacElroy, R. D. *J. Am. Chem. Soc.* **1983**, *105*, 2221.

(14) Williams, I. H. *J. Mol. Struc.* (*THEOCHEM*) **1983**, *94*, 275.

(15) Williams, I. H., manuscript in preparation.

Theoretical Probes of Activated-Complex Structure

J. Am. Chem. Soc., Vol. 107, No. 25, 1985 7719

to a standard state of 1 atm (cf. ref 16). Normal modes and vibrational frequencies were obtained by diagonalization of the mass-weighted Cartesian force-constant matrix.

Results and Discussion

Geometries. Parts a–e in Tables I contain the STO-3G optimized geometries of the reactants, activated complexes, and products for each of the reactions given in eq 1–5. Two diastereometric activated complexes, denoted cFFW‡ ("cis") and tFFW‡ ("trans"), were determined for hydration of formyl fluoride. The C–F and O_n–H_x bonds[17] were approximately synperiplanar and anticlinal, respectively (see Figure 1). Two isomeric activated complexes would similarly be expected for addition of water to acetaldehyde, but only that with eclipsed C–CH_3 and O_n–H_x bonds (cAW‡) is reported here. The coordinates of the substituent methyl group of cAW‡ and of the methanol–formaldehyde activated complex, FM‡ (and of the corresponding reactants and products), have been omitted from Table I for the sake of brevity, with the intension of facilitating comparison of geometrical changes accompanying each of the five related reactions.

The most obvious point concerning the geometries of the six activated complexes given in Table I and illustrated by Figure 1 is their extreme uniformity. The essentially coplanar four-membered ring, the out-of-plane location of the exocyclic H_x or C_x group, and the distortion from trigonal toward tetrahedral geometry about the electrophilic carbon atom are features which have been described in detail for FW‡ elsewhere[4] and which are preserved throughout this series of substituted activated complexes. The similarity of the activated complex geometries suggests that the structural requirements for concerted addition with proton transfer tend to outweigh any substituent effects. The concerted, four-center nature of these reactions is enforced by the non-existence of the zwitterionic species which would be involved in the alternative stepwise mechanism.[3]

Energetics. General Considerations. Total energies in STO-3G and in 4-31G at the STO-3G optimized geometry for each reactant, activated complex, and product species are listed in Table II. Potential energies of activation ($\Delta E^{\ddagger}$) and of overall reaction (ΔE) at the 4-31G//STO-3G level are given in Table III, together with Gibbs free energies of activation ($\Delta G^{\circ\ddagger}$) and of overall reaction (ΔG°) at 25 °C and 1 atm.

Since this is a modeling study, it is not our purpose to provide quantitative estimates of either the thermodynamics or kinetics of the reactions of eq 1–5. Instead, our aim is to examine the qualitative and semiquantitative effects of substituents on the properties of the activated complexes and, to some degree, on the energies of reaction and activation. Thus agreement with experiment was not aimed for. Nevertheless, it is comforting that the calculated Gibbs free energies of reaction are in general accord with such experimental observations as exist.[18] For example, a favorable equilibrium for addition of water or methanol to formaldehyde, but not to acetaldehyde, is indicated by the values of ΔG° in Table III.

Absence of Rate–Equilibrium Relationships. The Gibbs free energies of reaction and activation, shown in Table III, in principle provide the basis for a generalized Brønsted or Marcus relationship.[19] As Figure 2 shows, no such relationship exists, whether the free energies or potential energies of reaction and activation are used. While both the free energies of activation and of reaction vary considerably with substituent, there is no systematic relationship between the activation and the reaction thermodynamics (note that the range of free energies in each case is around 10 kcal/mol, corresponding to variations in rate or equilibrium
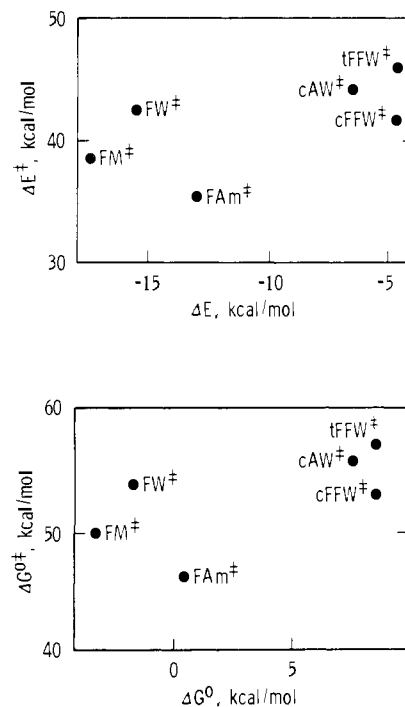

Figure 2. Potential energy of activation vs. potential energy of reaction (top panel) and Gibbs free energy of activation vs. Gibbs free energy of reaction (1 atm standard states, 298 K) (bottom panel).

constants at 300 K of around seven powers of ten).

The absence of a generalized Brønsted or Marcus relationship is particularly significant here, because the theoretical calculation corresponds to the gas phase, so that no involvement of solvation ("work terms") can explain the failure of the data to correlate. We also know that the reaction is truly concerted (we known even the form of the reaction-coordinate eigenvector) and that it occurs in one single elementary step.[20] Therefore, the failure of the relationship cannot arise from the participation of several steps in determining the rate or the presence of competitive reaction channels, as might have been the case in an experimental investigation.

In our view, the failure of the rate–equilibrium relationship derives from the fact that the activated complex is distant in structure from both reactants and products, possessing structural features not present in either the reactants or products. This is closely connected with the fact that the activation energy is large, and thus the activated complex is also distant in energy from both reactants and products. When the structure of the activated complex is such that its energetics are modeled by the reaction equilibrium energetics, a rate–equilibrium correlation should exist. Most simply, under these conditions the free-energy response of an activated complex to a particular reaction variable (substituent in this case) can be considered as a linear combination of the free-energy responses of the reactants and products.[21] When these conditions do not hold, no relationship can be expected. In the present case, the four-membered-ring structure of the activated complex introduces features not present in, and therefore not modeled by, the reactant and product molecules. A more detailed analysis of these features appears below.

Bond Orders. The bond distances for the bonds that make up the four-membered ring of the activated complexes (Table I) are intermediate between their reactant values and their product values. Obviously this corresponds to partial bonding, and it is desirable to employ a bond-order concept to discuss these features

(16) Williams, I. H.; Spangler, D.; Femec, D. A.; Maggiora, G. M.; Schowen, R. L. *J. Am. Chem. Soc.* **1983**, *105*, 31.

(17) The following notation is employed to indicate the atoms composing the activated complexes: atoms in the nucleophilic ("n") fragment: O_n, H_n, for the atoms in the four-membered ring, and H_x for the "external" hydrogen (and C_x for the "external" methyl of methanol); atoms in the formyl ("f") fragment: O_f, C, H_c ("cis" to H_x), H_t ("trans" to H_x).

(18) Bell, R. P. *Adv. Phys. Org. Chem.* **1966**, *4*, 1.

(19) Albery, W. J. *Annu. Rev. Phys. Chem.* **1980**, *31*, 227.

(20) In actual fact, the four-center reaction leads down to an activated complex for a bond rotation in the diol or aminol, but the energy involved in collapse of this species to a stable rotamer is so small as not to affect ΔE° or ΔG° sensibly. Thus this feature has no influence on the quality of the Brønsted–Marcus correlation.

(21) Leffler, J. E. *Science* **1953**, *117*, 340.

Table I. STO-3G Optimized Geometries for Reactants, Activated Complex, and Product of (a) $H_2O + CH_2O$, (b) $H_2O + CH_3CHO$, (c) $H_2O +$ FCHO, (d) $CH_3OH + CH_2O$, and (e) $NH_3 + CH_2O$

(a) $H_2O + CH_2O$

coordinate[a]	$H_2O + CH_2O$	FW‡	$CH_2(OH)_2$	coordinate[a]	$H_2O + CH_2O$	FW‡	$CH_2(OH)_2$
C-O$_n$		1.674	1.429	O$_n$-C-O$_f$		90.6	112.0
C-O$_f$	1.217	1.307	1.429	O$_n$-C-H$_c$		102.7	112.0
O$_n$-H$_n$	0.989	1.064		O$_n$-C-H$_t$		101.4	106.2
O$_f$-H$_n$		1.449	0.991	O$_f$-C-H$_c$	122.7	122.3	106.2
O$_n$-H$_x$	0.989	0.992	0.991	O$_f$-C-H$_t$	122.7	122.2	112.0
C-H$_c$	1.101	1.111	1.102	H$_c$-C-H$_t$	114.6	109.8	108.4
C-H$_t$	1.101	1.109	1.102	C-O$_n$-H$_n$		75.5	
				C-O$_n$-H$_x$		114.7	104.0
				H$_x$-O$_n$-H$_n$	100.0	109.9	
				O$_n$-H$_n$-O$_f$		115.5	
				O$_f$-C-O$_n$-H$_n$		-0.0	
				ω^b	0.0	22.0	55.8

(b) $H_2O + CH_3CHO$

coordinates[a]	$H_2O + CH_3CHO$	cAW‡	$CH_3CH(OH)_2$	coordinates[a]	$H_2O + CH_3CHO$	cAW‡	$CH_3CH(OH)_2$
C-O$_n$		1.691	1.432	O$_n$-C-O$_f$		89.8	112.0
C-O$_f$	1.217	1.308	1.432	O$_n$-C-C$_c$		106.7	111.9
O$_n$-H$_n$	0.989	1.066		O$_n$-C-H$_t$		99.7	105.7
O$_f$-H$_n$		1.431	0.992	O$_f$-C-C$_c$	124.3	121.0	111.9
O$_n$-H$_x$	0.989	0.991	0.992	O$_f$-C-H$_t$	121.5	122.2	105.7
C-C$_c$	1.537	1.554	1.555	C$_c$-C-H$_t$	114.2	110.3	109.2
C-H$_t$	1.104	1.111	1.100	C-O$_n$-H$_n$		74.7	
				C-O$_n$-H$_x$		115.2	104.7
				H$_x$-O$_n$-H$_n$	100.0	109.6	
				O$_n$-H$_n$-O$_f$		116.6	
				O$_f$-C-O$_n$-H$_n$		-0.5	
				ω^b	0.0	23.4	56.0

(c) $H_2O +$ FCHO

coordinate[a]	$H_2O +$ FCHO	cFFW‡	tFFW‡	FCH(OH)$_2$	coordinate[a]	$H_2O +$ FCHO	cFFW‡	tFFW‡	FCH(OH)$_2$
C-O$_n$		1.668	1.672	1.423	O$_n$-C-O$_f$		90.3	90.0	113.2
C-O$_f$	1.210	1.301	1.301	1.423	O$_n$-C-H		103.1	103.7	107.0
O$_n$-H$_n$	0.989	1.072	1.073		O$_n$-C-F		102.9	103.1	109.2
O$_f$-H$_n$		1.420	1.413	0.992	O$_f$-C-H	125.6	124.2	123.9	107.0
O$_n$-H$_x$	0.989	0.991	0.990	0.992	O$_f$-C-F	122.1	120.0	120.3	109.2
C-F	1.351	1.366	1.360	1.379	F-C-H	112.3	109.3	109.1	111.0
C-H	1.108	1.116	1.119	1.108	C-O$_n$-H		74.8	74.5	
					C-O$_n$-H$_x$		113.9	114.4	104.7
					H$_x$-O$_n$-H$_n$	100.0	110.5	110.4	
					O$_n$-H$_n$-O$_f$		116.0	116.4	
					O$_f$-C-O$_n$-H$_n$		-1.6	0.3	
					ω^b	0.0	23.2	23.5	56.7

(d) $CH_3OH + CH_2O$

coordinate[a]	$CH_3OH + CH_2O$	FM‡	CH_3OCH_2OH	coordinate[a]	$CH_3OH + CH_2O$	FM‡	CH_3OCH_2OH
C-O$_n$		1.681	1.432	O$_n$-C-O$_f$		90.1	112.5
C-O$_f$	1.217	1.304	1.428	O$_n$-C-H$_c$		102.8	111.7
O$_n$-H$_n$	0.991	1.067		O$_n$-C-H$_t$		101.6	105.7
O$_f$-H$_n$		1.446	0.991	O$_f$-C-H$_t$	122.7	122.2	106.5
O$_n$-C$_x$	1.433	1.440	1.435	O$_f$-C-H$_t$	122.7	122.2	111.8
C-H$_c$	1.101	1.110	1.101	H$_c$-C-H$_t$	114.6	110.0	108.6
C-H$_t$	1.101	1.109	1.102	C-O$_n$-H$_n$		75.6	
				C-O$_n$-C$_x$		122.3	110.2
				C$_x$-O$_n$-H$_n$	103.9	115.8	
				O$_n$-H$_n$-O$_f$		115.1	
				O$_f$-C-O$_n$-H$_n$		1.2	
				ω^b	0.0	21.8	55.7

(e) $NH_3 + CH_2O$

coordinate[a]	$NH_3 + CH_2O$	FAm‡	NH_2CH_2OH	coordinate[a]	$NH_3 + CH_2O$	FAm‡	NH_2CH_2OH
C-N		1.728	1.487	N-C-O		91.8	110.1
C-O	1.217	1.315	1.427	N-C-H$_c$		102.6	107.4
N-H$_n$	1.032	1.116		N-C-H$_t$		102.6	113.3
O-H$_n$		1.461	0.990	O-C-H$_c$	122.7	122.2	111.8
N-H$_x$	1.032	1.035	1.032	O-C-H$_t$	122.7	122.2	106.5
C-H$_c$	1.101	1.110	1.100	H$_c$-C-H$_t$	114.6	108.8	107.9
C-H$_t$	1.101	1.110	1.100	C-N-H$_n$		72.7	
				C-N-H$_x$		120.4	107.8
				H$_x$-N-H$_n$	104.2	116.2	
				N-H$_n$-O		117.1	
				O-C-N-H$_n$		0.0	
				ω^b	0.0	23.9	56.0

^{a} Bond lengths in Å, angles in deg; see Figure 1 for labeling of coordinates. ^{b} Out-of-plane angle between C-O$_f$ and H$_c$-C-H$_t$.

Table II. Total Energies for Reactant, Activated Complex, and Product Species[a]

species	symmetry	STO-3G// STO-3G[d]	4-31G// STO-3G[d]
H_2O	C_{2v}	-74.96590	-75.90333
CH_2O	C_{2v}	-112.35435	-113.69171
CH_3CHO	C_s	-150.94599	-152.68499
FCHO	C_s	-209.80379	-212.44287
CH_3OH	C_s	-113.54919	-114.86719
NH_3	C_{3v}	-55.45542	-56.09839
FW‡	C_1	-187.25296	-189.52663
cAW‡	C_1	-225.84207	-228.51757
cFFW‡	C_1	-284.73491	-288.27930
tFFW‡	C_1	-284.73284	-288.27264
FM‡	C_1	-225.83782	-228.49715
FAm‡	C_s	-167.72772	-169.73340
$CH_2(OH)_2$[b]	C_2	-187.38941	-189.61980
$CH_3CH(OH)_2$[c]	C_s	-225.97227	-228.59881
$FCH(OH)_2$[c]	C_s	-284.85798	-288.35361
CH_3OCH_2OH[b]	C_1	-225.97250	-228.58648
NH_2CH_2OH[b]	C_1	-167.86778	-169.81064

[a] Energies in hartrees (1 hartree = 627.5 kcal mol^{-1}). [b] (+sc,+sc) conformer. [c] (+sc,-sc) conformer. [d] Total energy in STO-3G optimized geometry. [e] Total energy in 4-31G at STO-3G optimized geometry.

Table III. Calculated Energy Changes for Carbonyl Addition[a]

reaction	activated complex	activation energy $\Delta E^{\ddagger}$	$\Delta G^{\circ\ddagger}$	reaction energy ΔE	ΔG°
$H_2O + CH_2O$	FW‡	42.9	54.1	-15.5	-1.6
$H_2O + CH_3CHO$	cAW‡	44.4	56.2	-6.6	7.6
$H_2O + FCHO$	cFFW‡	42.0	53.5	-4.7	7.6
	tFFW‡	46.2	57.6		
$CH_3OH + CH_2O$	FM‡	38.8	50.0	-17.3	-3.0
$NH_3 + CH_2O$	FAm‡	35.6	46.4	-13.0	0.6

[a] Potential energies of activation ($\Delta E^{\ddagger}$) and of reaction (ΔE) are 4-31G//STO-3G values given in Table II; Gibbs free energies of activation ($\Delta G^{\circ\ddagger}$) and of reaction (ΔG°) are thence evaluated according to eq 6 with STO-3G vibrational frequencies and geometries; all energies are in kcal mol^{-1}, and the Gibbs free energies refer to a standard state of 1 atm at 25 °C.

quantitatively. Various quantum-mechanical bond-order definitions might have been used for this purpose, but our aim of providing theoretical models for mechanistic investigations suggests that the Pauling bond order[22] B (eq 7) is a more useful choice. In eq 7, $R(B)$ and $R(1)$ are respectively the lengths of bonds of order B and order unity.

$$B = \exp\{[R(1) - R(B)]/0.3\} \qquad (7)$$

Pauling bond orders have been used with some frequency in mechanistic studies.[23] In empirical modeling of the relationship between activated complex structure and the magnitudes of kinetic isotope effects, the use of the Pauling bond order is now standard.[24] The BEBO kinetic theory of Johnston and his co-workers[25] introduced the concept for the description of activated complexes. Implicitly or explicitly, it is commonly employed in converting measures of "reaction progress at the activated complex", such as the slopes of linear free-energy correlations, to structural characteristics of activated complexes. The same, largely implicit usage is general for considerations based on the normalized reaction diagrams[26] called MARs or maps of alternate routes by Bruice.[27] Because of this general usage of the concept, we will

(22) Pauling, L. *J. Am. Chem. Soc.* **1947**, *69*, 542.
(23) Burton, G. W.; Sims, L. B.; Wilson, J. C.; Fry, A. *J. Am. Chem. Soc.* **1977**, *99*, 3371.
(24) Sims, L. B. *Isotopes Org. Chem.*, in press.
(25) Johnston, H. S. "Gas Phase Reaction Rate Theory"; Ronald Press: New York, 1966.
(26) Jencks, W. P. *Chem. Rev.* **1972**, *72*, 705.
(27) Bruice, T. C. *Annu. Rev. Biochem.* **1976**, *72*, 705.

convert the bond distances of Table I into Pauling bond orders for discussion of partial bonding in the activated complexes. To maintain self-consistency, values of $R(1)$ for the various bonds have been taken from the calculated structures of methanediol and aminomethanol (C–O, 1.429 Å; O–H, 0.991 Å; C–N, 1.487 Å; N–H, 1.032 Å). The values of B for the making and breaking of bonds in the activated complexes are shown in Figure 1.

Reaction Progress at the Activated Complex. Some of the most important mechanistic generalizations now in use attempt to deal with the question of the reaction progress at the activated complex for various component processes involved in the transformation of reactants into products. We shall consider the reactions of eq 1–5 as involving two component processes: PT, or proton transfer (the transfer of the proton from the nucleophilic reactant to the formyl oxygen); and HAR, or heavy-atom reorganization (the formation of the carbon–nucleophile bond and the concomitant fission of the formyl π-bond).

The eigenvectors for the reaction coordinates, shown in Figure 1, demonstrate that these two component processes are coupled, or concerted.[28] That is, the motions of the individual atoms are such that transfer of the proton, formation of the new σ-bond, and fission of the π-bond are all occurring to some extent in the reaction-coordinate motion.

The simplest consideration of potential energy surface topography, following Hammond's postulate,[29] would predict that "reaction progress" at the activated complex would be slightly less than 50% in these reactions which (despite having large activation energies) are somewhat exothermic. Progress toward tetrahedrality about the formyl carbon C, measured by the fractional change in the angle ω (Table I), yields a "reaction progress" value of ~40% for each activated complex. The bond-order data given in Figure 1 suggest that the new σ-bond to the nucleophile has been formed and the π-bond of the formyl group broken to ~45%. Thus HAR and the angular change at C are in accord with the Hammond-postulate prediction. However, PT has occurred only to the extent of ~25% as judged by the bond orders for the activated complexes. There is thus an "imbalance"[30] between the component processes, with PT lagging behind HAR.

Orbital Interactions and Reaction Progresses. The somewhat "reactant-like" character (reaction progress 25–45%) of the activated complexes suggests that a qualitative explanation of the imbalance between HAR and PT be sought by considering the interactions between reactant orbitals as the reaction partners approach each other and enter the activated complex. HAR is initiated by donation of a nucleophile lone pair of electrons from an n nonbonding orbital into the π^* antibonding orbital of the carbonyl group. The n and π^* orbitals lie relatively close in energy and should interact favorably. In contrast, PT is initiated by donation of the π bonding electron pair of the carbonyl group into the σ^* antibonding orbital of the $O_n–H_n$ or $N–H_n$ bond of the nucleophile. These orbitals are distant in energy and should interact less favorably.

Thus both HAR and PT in this exothermic reaction are advanced to a degree less than 50%, as expected on the basis of a "parallel effect".[31] As judged by reactant frontier orbital interactions, the more facile of these component processes, HAR, is more advanced (~45%) than the less facile, PT (~25%). This is as expected on the basis of "perpendicular effects".[31] These features are readily understood in terms of the topological properties of the MARs referred to above.

Qualitative Location of Activated Complex Structures on MARs. Figure 3 shows the form of an MAR in which two component processes (plotted on the ordinate and abscissa) are taken to contribute to overall reaction progress. The expected structure of the activated complex may be located on this diagram by considering (i) "parallel" effects and (ii) "perpendicular" effects.

(28) Gandour, R. D.; Maggiora, G. M.; Schowen, R. L. *J. Am. Chem. Soc.* **1974**, *96*, 6967.
(29) Hammond, G. S. *J. Am. Chem. Soc.* **1955**, *77*, 334.
(30) Maggiora, G. M.; Schowen, R. L. In "Bioorganic Chemistry"; van Tamelen, E. E., Ed.; Academic Press: New York, 1977; Vol. 1.
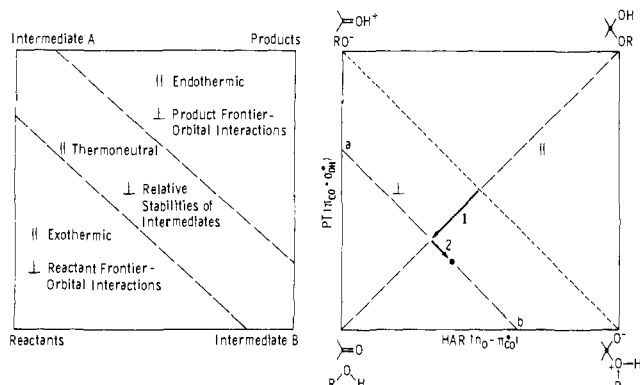(31) Thornton, E. R. *J. Am. Chem. Soc.* **1967**, *89*, 2915.

Figure 3. Maps of alternative routes (MARs) for reactions described by two component processes. The left panel illustrates a division of the map into three regions characterized by exothermic, roughly thermoneutral, and endothermic reactions. This overall reaction energy thus determines the approximate location of an activated complex along the "parallel" axis ($\parallel$) between the reactant and product corners. In each region the position of an activated complx along the "perpendicular" axis ($\perp$) is then determined as indicated. The right panel illustrates the application of this protocol for location of activated complexes for the concerted carbonyl additions presently considered. See text for details. Note that these MARs are schematic diagrams only: no information is implied regarding actual potential energy surfaces or explicit geometrical coordinates.

First, the relative stabilities of reactants and products are used to locate the structure along the "parallel" axis connecting the reactant corner with the product corner: an exothermic reaction yields an "early transition state" (reaction progress less than 50%) and an endothermic reaction a "late transition state" (reaction progress greater than 50%). Next, a second axis perpendicular to the first is passed through the point just located and the expected structure of the activated complex is found by moving along this axis. Now the pertinent consideration is the relative energy of the two points at the intersections of this "perpendicular" axis with the edges of the diagrams. The expected structure of the activated complex lies closer to the more stable of the intersection points. For a roughly thermoneutral reaction, the intersections are the two corners corresponding to the intermediates in the two possible stepwise versions of the reaction. For "early transition states" or "late transition states", the situation is less simple.

We suggest that an appropriate procedure is to use a frontier orbital approach qualitatively to order the energies of the intersection points. For an "early transition state", the reactant frontier orbital interactions will be appropriate and for a "late transition state" the interactions of the product frontier orbitals. This procedure is summarized in the left-hand panel of Figure 3 and specifically applied to the present case in the right-hand panel.

The carbonyl-addition reactions are all exothermic by as much as 17.3 kcal mol^{-1}. Thus the reaction progress along the parallel axis should be less than 50%, as depicted by vector **1**. Since the expected activated-complex structure is therefore "reactant-like", the reactant frontier orbital interactions for PT and HAR are used, as above, to order the energies of the intersection points of the perpendicular axis at (a) and (b). The more favorable $n_O-\pi_{CO}^*$ interaction for HAR, vs. the less favorable $\pi_{CO}-\sigma_{OH}^*$ interaction for PT, gives the direction of vector **2**, leading to an approximae location for the activated-complex structure (heavy black dot). This corresponds qualitatively to the finding that reaction progress for HAR is advanced to $\sim$45% and that for PT to $\sim$25%.

Convervation of Bond Order? Apparently there is approximate conservation of bond order about the transferring hydrogen H_n (total bond order $\sim$1) and about the formyl carbon C (total bond order $\sim$2) in the four-membered ring of the activated complexes. About the oxygen O_n or nitrogen N at the nucleophilic center, the total bond order in the activated complexes is $\sim$20% greater than in the reactants, whereas at the opposite corner of the ring there is a deficiency of $\sim$25% in the total bond order about the formyl oxygen O_f in the activated complexes. The excess of bond order at the nucleophile oxygen or nitrogen corresponds, it should be noted, to a *decrease* in electron density at this center: the

Table IV. Analysis of 4-31G//STO-3G Potential Energies of Activation[a]

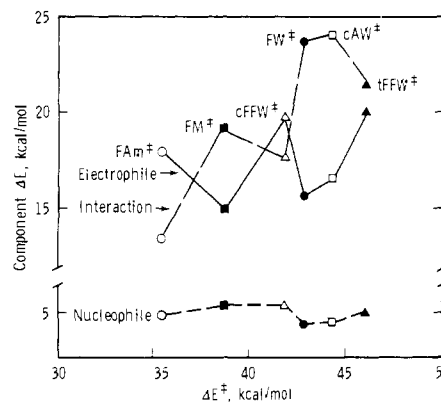| reaction	activated complex	ΔE_{DIST}(nuc)	ΔE_{DIST}(elec)	ΔE_{INT}
$H_2O + CH_2O$	FW‡	4.1	15.4	23.5
$H_2O + CH_3CHO$	cAW‡	4.2	16.3	23.9
$H_2O + FCHO$	cFFW‡	4.9	19.6	17.5
	tFFW‡	5.0	19.9	21.3
$CH_3OH + CH_2O$	FM‡	5.0	14.8	19.0
$NH_3 + CH_2O$	FAm‡	4.4	17.9	13.3

[a] All energies in kcal mol^{-1}.

Figure 4. Distortion analysis of the potential energies of activation. The abscissa gives the total potential energies of activation. Energy components derived from the distortion analysis are plotted on the ordinate: distortion energy for the electrophilic partner (points connected by a solid line); distortion energy for the nucleophilic partner (points connected by short dashes); interaction energy of the distorted nucleophilic and electrophilic partners (points connected by long dashes).

electrons of the reactant atom are donated in the activated complex to *both* H_n (bond order $\sim$0.75) and C (bond order $\sim$0.45). Similarly, the deficiency of bond order at O_f corresponds to an excess of electron density. There is thus, in the activated complex, a charge distribution (relatively positive O_n or N, relatively negative O_f) not far from that of the zwitterion, the "avoided intermediate" in this enforcedly concerted reaction. We have pointed out this resemblance earlier.[3]

The prediction of approximate bond-order conservation at H_c and C—the centers undergoing quasinucleophilic displacement—in these minimal-basis calculations does not provide unequivocal support for a general principle of bond-order conservation in this type of process. The present results may be consequent upon the use of a small basis set. For example, the strict conservation of unit bond order at H_n may derive from the presence of only one basis function on H_m, forcing the electron density into the internuclear regions about this atom. With larger basis sets[4] the total bond order about H_n in the activated complex FW‡ drops to $\sim$0.8.

Distortion–Interaction Analysis of Activated Complex Formation. We have previously[16] employed an analysis of the activation energetics for reactions such as this, in which the net energy of activation is dissected by individual calculation of the components into contributions from (i) distortion of the nucleophile into its activated-complex configuration, (ii) distortion of the electrophile into its activated-complex configuration, and (iii) interaction of these two distorted fragments to generate the actual activated complex. Potential energy is employed in this analysis instead of free energy because the free energy contains contributions, such as the entropy of combination of the two reactants, which do not instructively add to this kind of analysis (cf. ref 16).

The data are presented in Table IV and can be appreciated by examining Figure 4. The total potential energy of activation, ranging from 35.6 kcal mol^{-1} (for FAm‡) to 46.2 kcal mol^{-1} (for tFFW‡), is analyzed into (i) a contribution from distortion of the nucleophile (i.e., water, methanol, or ammonia) which is essentially small and constant at 4–5 kcal mol^{-1}, (ii) a contribution from distortion of the electrophile (i.e., the formyl moiety) of sub-

Table V. Selected Vibrational Frequencies for Activated Complexes from Scaled STO-3G Force Constants

mode[a]	FW‡	cAW‡	cFFW‡	tFFW	FM‡	FAm‡
O_n-H_x stretch	3506	3509	3502	3511		
$H_n-O_n-H_x$ bend	1516	1536	1491	1505		
$C-O_n-H_x$ bend	727	773	820	837		
O_n-H_x wag	450	470	449	435		
CH_2 scissor	1569				1574	1569
CH_2 twist	1085				1019	1066
CH_2 rock	962				866	988
C–H stretch	2927	2872	2874	2841	2932	2910
	2832				2839	2826
O_n-H_n stretch	2488	2456	2445	2432	2482	2347[b]
$C-O_f$ stretch	1327	1472	1524	1513	1330	1169
C–H wag	1191	1141	1051	1064	1190	1290
rhomboidal ring def.	904	906	913	909	785	858
trapezoidal ring. def.	611	607	663	630	611	542
decomp mode	i1343	i1348	i1354	i1366	i1320	i1475

[a] Approximate description of normal mode. [b] $N-H_n$ stretch.

stantially larger magnitude which varies in an irregular manner, and (iii) a contribution from interaction of the distorted fragments which (at least in this series) also varies in an irregular manner.

These components of the activation energy are quantitatively sensitive to the size of the basis set and the omission of correlation effects, so that detailed consideration of absolute magnitudes is not justified. There is no reason to suspect that the *trends* are in error, however (cf. earlier discussion).

The small and constant component ΔE_{DIST}(nuc) is in accord with the fact that structural distortion is small for all the nucleophiles. This is readily confirmed from the bond orders given in Figure 1: the O–H and N–H bonds of the nucleophile have been extended by only about 25% (bond orders $\sim$0.75).

The electrophile distortion energies and the interaction energies are both large and together make up most of the activation energy. The irregular variation of ΔE_{DIST}(elec) is not surprising in view of the unique characteristics of each of the electrophile structures. These unique features, as well as the similarly unique characteristics of the three nucleophiles, also contribute to the irregular variation of the interaction energies. Any apparent relationship in the trends of electrophile distortion energy vs. interaction energy doubtless stems from a complicated superposition of effects: e.g., actual compensation (in which greater distortion leads to reactant delocalization energy) and hydrogen-bond formation in the activated complex.

Force Constants. Diagonal "symmetry" force constants for each of the activated complexes were obtained from the computed Cartesian force constants (as described elsewhere[32]). The numerical values for FW‡ have been given previously.[4] These force-constant values are not independent of the choice of coordinates and thus may be compared with each other only because similar sets of coordinates were used for the various activated complexes. It was found that just as the geometries of the activated complexes were very similar, so also were their force constants.

Vibrational frequencies and approximate descriptions of the normal modes for the various activated complexes are presented in Table V. Comparison of frequencies for the different species is meaningful only to the extent that the normal modes are the same. The O_n-H_x stretching frequencies of all activated complexes except FAm‡ have nearly the same value because the diagonal O_n-H_x stretching force constants and the "O_n-H_x" normal coordinates are virtually the same for each activated complex. On the other hand, the $C-O_n-H_x$ bending frequencies show substantial variation; this is because the normal coordinate described as "$C-O_n-H_x$ bending" is a different combination of the $C-O_n-H_x$ valence coordinate and other coordinates (particularly that for twisting about carbon) in each structure. The $C-O_f$ stretching frequencies show considerable variation across the range of ac-

tivated complexes. The low frequency in FAm‡ seems to be due to a small force constant for this stretching coordinate, but the variation in the $C-O_f$ frequencies cannot be accounted for by changes in diagonal force constants alone. It may be possible to resolve these questions by examination of "relaxed" force constants.[32]

The decomposition mode, depicted in Figure 1 for each activated complex, is composed predominantly of PT between the nucleophile and the carbonyl oxygen atom, together with motion toward tetrahedrally about the carbonyl carbon atom. Both the nature of this mode and the value of its associated imaginary frequency are remarkably similar for all the structures.

The kinetic consequences of shifts in activated complex vibrational frequencies resulting from isotopic substitution in each of these activated complexes will be considered in a later publication.

Summary and Conclusions

These examples of four-center carbonyl-addition reactions exhibit activated complex structures which are remarkably unaffected by changes in substitution. In spite of this, the activation energies vary considerably. In all cases, the reaction-coordinate eigenvectors show the proton-transfer (PT) component of the reaction to be coupled to the heavy-atom reorganization (HAR) component so that the reactions are truly concerted. As expected for reactions in which activated complex properties cannot be modeled adequately by reactant and product properties, no rate–equilibrium relationships are found.

The overall reaction progress and progress in each of the component processes (i.e., the location of the activated complex on a MAR) can be deduced from the expected parallel and perpendicular effects. According to the parallel effect, these exothermic reactions should have a degree of reaction progress less than 50% at the activated complex. The perpendicular effect can then be deduced from a consideration of reactant frontier orbital interactions: HAR requires an n–π* interaction, which is relatively favorable, while PT requires a π–σ* interaction, which is relatively less favorable. HAR should then be more advanced and PT less. This is as found (HAR, $\sim$45%; PT, $\sim$25%).

From the reaction progress in HAR and PT some energetic features of the reaction may be deduced. PT is only 25% advanced, suggesting little geometrical distortion of the nucleophilic proton donor at the activated complex and little energy cost from nucleophile distortion. In fact this cost is only 4–5 kcal mol^{-1}. HAR is advanced 45% and, as expected, the electrophile distortion is larger and more costly at 15–20 kcal mol^{-1}.

Like the geometries, the force fields and vibration frequencies, including the imaginary frequency for reaction-coordinate motion, are similar for all the activated complexes.

(32) Williams, I. H. *Chem. Phys. Lett.* **1982**, *88*, 462.